Geophysical Research Letters

RESEARCH LETTER
10.1029/2018GL081462

# Global Mean Surface Temperature Response to Large-Scale Patterns of Variability in Observations and CMIP5

**Jules B. Kajtar[1], Matthew Collins[1], Leela M. Frankcombe[2,3], Matthew H. England[2,3], Timothy J. Osborn[4], and Marcus Juniper[1]**

[1]College of Engineering, Mathematics, and Physical Sciences, University of Exeter, Exeter, UK, [2]Australian Research Council's Centre of Excellence for Climate Extremes, Australia, [3]Climate Change Research Centre, University of New South Wales, Sydney, New South Wales, Australia, [4]Climatic Research Unit, School of Environmental Sciences, University of East Anglia, Norwich, UK

**Abstract** Global mean surface temperature (GMST) fluctuates over decadal to multidecadal time scales. Patterns of internal variability are partly responsible, but the relationships can be conflated by anthropogenically forced signals. Here we adopt a physically based method of separating internal variability from forced responses to examine how trends in large-scale patterns, specifically the Interdecadal Pacific Oscillation (IPO) and Atlantic Multidecadal Variability (AMV), influence GMST. After removing the forced responses, observed variability of GMST is close to the central estimates of Coupled Model Intercomparison Project phase 5 simulations, but models tend to underestimate IPO variability at time scales >10 years, and AMV at time scales >20 years. Correlations between GMST trends and these patterns are also underrepresented, most strongly at 10- and 35-year time scales, for IPO and AMV, respectively. Strikingly, models that simulate stronger variability of IPO and AMV also exhibit stronger relationships between these patterns and GMST, predominately at the 10- and 35-year time scales, respectively.

**Plain Language Summary** Despite the smooth and steady increase of greenhouse gas concentrations, the rate of global warming has not been as stable over the past century. There are periods of stronger warming, or even slight cooling, in the global mean temperature record, which can persist for several years or longer. These changes have been linked to regional climate patterns, most notably within the Pacific and Atlantic Ocean climate systems. Climate models do not exhibit the same level of variations in these Pacific and Atlantic oscillations as compared to the observed record, and the connections between these oscillations and the global temperature are also diminished. However, there is a tendency for those models that show stronger Pacific and Atlantic oscillations to also exhibit stronger relationships between these patterns and global temperature changes.

**Key Points:**
- Interdecadal Pacific Oscillation and Atlantic Multidecadal Variability are weaker than observed in state-of-the-art models
- Correlations between these patterns and global temperature changes are identified, but these too are weaker in models
- Models that exhibit stronger variability in these patterns also exhibit stronger relationships between the patterns and global temperature

**Supporting Information:**
- Supporting Information S1

**Correspondence to:**
J. B. Kajtar,
j.kajtar@exeter.ac.uk

**Citation:**
Kajtar, J. B., Collins, M., Frankcombe, L. M., England, M. H., Osborn, T. J., & Juniper, M. (2019). Global mean surface temperature response to large-scale patterns of variability in observations and CMIP5. *Geophysical Research Letters*, *46*, 2232–2241. https://doi.org/10.1029/2018GL081462

Received 26 NOV 2018
Accepted 29 JAN 2019
Accepted article online 30 JAN 2019
Published online 18 FEB 2019



## 1. Introduction

Anthropogenic greenhouse gases have been responsible for global warming over the last century, but a range of drivers have contributed to variations in the observed global mean surface temperature (GMST) across a range of time scales. The slowdown in global warming during the early twenty-first century, sometimes referred to as the "hiatus," has garnered extensive research. Numerous mechanisms have been proposed for the slowdown (see Medhaug et al., 2017 for a comprehensive review), but many argue that particular patterns of internal climate variability drove the weaker GMST trend. For example, the negative phase of the Interdecadal Pacific Oscillation (IPO) appears to have played a role in the slowdown (England et al., 2014; Kosaka & Xie, 2013; Watanabe et al., 2014), and the strength of the negative IPO may have in part been enhanced by a strong Atlantic warming trend (Chikamoto et al., 2016; Li et al., 2016; McGregor et al., 2014).

The association of the global warming slowdown with internal variability has motivated this study on the extent to which large-scale patterns of variability drive decadal or multidecadal trend changes in GMST, in both observations and models. The common view is that the Pacific Ocean plays a substantial role in modulating GMST. As already noted, the IPO is thought to be tied to decadal-scale GMST trend changes (Dai et al., 2015; England et al., 2014; Henley & King, 2017; Kosaka & Xie, 2016; Maher et al., 2014; Meehl et al., 2016). However, Atlantic Multidecadal Variability (AMV) has also been linked with GMST changes (Chylek et al., 2016; Mann et al., 2014; Pasini et al., 2017; Wang et al., 2017), as have the AMV in combination with Pacific variability (Dong & Zhou, 2014; Nagy et al., 2017; Steinman et al., 2015; Stolpe et al., 2017; Yao

et al., 2016). The Indian (Luo et al., 2012) and Southern Oceans (Oka & Watanabe, 2017) may also play a role. This study focuses on the two dominant patterns of internal variability at decadal and multidecadal time scales: the IPO and AMV.

Central to the analysis of GMST variations is the separation of internal variability and forced response. The simplest method of excluding the anthropogenic greenhouse gas forcing signal is to remove a linear trend, but this introduces spurious signals, as the forced response is not linear (Frankcombe et al., 2015; Mann et al., 2014). Another approach is to subtract a global mean sea surface temperature (SST) time series (e.g., Douville et al., 2015; Farneti, 2017; Lyu & Yu, 2017; Trenberth & Shea, 2006), but again, this is problematic, since it removes a component of desired internal variability. In this study, an approach based on the response in multiple model simulations is adopted (Allen & Stott, 2003; Frankcombe et al., 2015; Mann et al., 2014; Schurer et al., 2013; Steinman et al., 2015). This approach removes an estimate of responses to forcings that are common across the model ensemble, that is, anthropogenic greenhouse gas and aerosol forcing, as well as volcanic aerosol forcing.

With an estimate of the forced response removed, the performance of the Coupled Model Intercomparison Project phase 5 (CMIP5) historical experiments in simulating the observed variability in GMST, the IPO, and AMV, at a range of interdecadal to multidecadal time scales, is assessed. Correlations are then computed between these three indices, again at a range of time scales, to determine the extent to which large-scale patterns of variability may imprint on GMST.

## 2. Data

The analysis of GMST, IPO, and AMV is conducted over the period 1880 to 2017. The HadISST v1.1 sea surface temperature (Rayner et al., 2003) is analyzed together with the HadCRUT v4.5.0.0 surface air temperature (Morice et al., 2012). The observed relationships are compared to the historical simulations in CMIP5. Most historical simulations were run to 2005, and thus, they are extended here to 2017 with the Representative Concentration Pathway (RCP) 8.5 (Riahi et al., 2011) simulations. The choice of RCP extension does not make a significant difference for the early period of the twenty-first century (e.g., Collins et al., 2013; England et al., 2015). The two CMIP5 variables analyzed herein are SST (CMIP5 variable name: *tos*) and surface air temperature (*tas*). The available ensemble members are listed in Table S1.

The IPO is characterized by the tripolar index (TPI; Henley et al., 2015), defined as $\mathrm{TPI} = T_C - \frac{1}{2}(T_N + T_S)$, where the terms represent SST area averages over the central Pacific, $T_C$ : $10^{\circ}\mathrm{S} - 10^{\circ}\mathrm{N}$, $170^{\circ}\mathrm{E} - 90^{\circ}\mathrm{W}$; the north Pacific, $T_N$ : $25^{\circ} - 45^{\circ}\mathrm{N}$, $140^{\circ}\mathrm{E} - 145^{\circ}\mathrm{W}$; and the south Pacific, $T_S$ : $50^{\circ} - 15^{\circ}\mathrm{S}$, $150^{\circ}\mathrm{E} - 160^{\circ}\mathrm{W}$. AMV is represented by the area-averaged SST over the North Atlantic region of $5^{\circ} - 60^{\circ}\mathrm{N}$, $80^{\circ}\mathrm{W} - 10^{\circ}\mathrm{W}$ (Knight, 2009). GMST is simply the global weighted average of surface air temperature. Blended air and sea surface temperatures (Cowtan et al., 2015) were also tested, but these made negligible differences to the findings.

## 3. Methods

Removing the externally forced response from the data is a key component of this study, so that the patterns of internal variability can be accurately identified. A method based on "optimal fingerprinting" is used (Allen & Stott, 2003; Frankcombe et al., 2015, 2018; Mann et al., 2014; Schurer et al., 2013; Steinman et al., 2015). In this approach, the forced response is estimated from an ensemble of model experiments, following the single-factor scaling method of Frankcombe et al. (2015). Details are given in the supporting information (Text S1). Our approach differs from Frankcombe et al. (2015) and Allen and Stott (2003) in that the estimated forced signal is always taken to be the multimodel mean of the CMIP5 historical GMST (Figure S1a, black curve), regardless of whether removing the forced response from an SST index, grid-point SST data, or GMST. The multimodel mean GMST is scaled before subtraction from the raw time series in each model simulation and the observed data (Text S1).

Several choices could have been made in the forced response removal process (Text S1), but ultimately, there is no perfect method for the analysis of multiple model simulations together with observations. The simplest approach in this regard has been adopted here, which is to treat each realization independently. However,

the approach here is nevertheless a substantial improvement over linear or quadratic detrending (Frankcombe et al., 2015; Mann et al., 2014; Steinman et al., 2015).

Another caveat to this analysis is that the real-world forcings for 2006–2017 have turned out to be different to those applied to the RCP8.5 experiments which were used to extend the historical simulations to 2017 (Schmidt et al., 2014). For example, the forecast of volcanic forcing, which is thought to be a component driving the early 2000s global warming slow-down, was too weak in the RCP scenarios (Huber & Knutti, 2014; Santer et al., 2014; Smith et al., 2016; Vernier et al., 2011). Therefore, the multimodel mean forced signal for the period following 2006 may not deliver the best estimate for the analysis of the observed record. This effect is nevertheless small, especially since the period of analysis stretches back to 1880.

The following analysis is largely of multiyear running trends (Text S2) of annual mean data (Figures S1a–S1c) after the forcing response has been removed (Figures S1d–S1f). All quoted values of correlations are the Pearson's linear correlation coefficient.

## 4. Results

### 4.1. Standard Deviation of GMST, IPO, and AMV Trends

We inspected the standard deviation of running trends of GMST, and the IPO and AMV indices, over a range of time scales (Figures 1a–1c). Here and from this point on, the forced response has been removed from all time series. Although there is a large range in the standard deviation of simulated GMST trends, the observed standard deviations are close to the multimodel mean values across most time scales (Figure 1a; Flato et al., 2013; Marotzke & Forster, 2015). The model-mean standard deviation is slightly larger than in observations for ~5- to 15-year running trends, but nevertheless, the observations lie within the central 68% of the model range for all time scales. Larger differences are seen for the IPO and AMV. For the IPO, the observations diverge from the model mean at >10-year running trends (Figure 1b). Beyond 20-year trends, the observed standard deviation is stronger than in a substantial proportion of models, lying well outside the central 68% model range. These findings are consistent with Henley et al. (2017). Standard deviation of AMV index trends in observations and models shows better agreement for 10-year trends, but again, observed standard deviation is larger at longer time scales (Figure 1c; although the standard deviations become more uncertain for these longer windows as there are fewer independent trends). Unlike the observations, the standard deviation across models tends to diminish for longer running trends (in agreement with Cheung et al. (2017)).

There is debate in the literature surrounding the origins of AMV. The common view is that AMV is driven mainly by processes internal to the Atlantic climate system, but recent studies reported evidence that external forcing, such as anthropogenic aerosol emissions, also have an influence (see Vecchi et al. (2017) for a summary of these views and supporting references). To test whether the process of removing the forced response also removes a component of AMV, the piControl experiments were analyzed, after accounting for model drift (Text S1; Sen Gupta et al., 2013). Following the present procedure of forced response removal in the historical experiments, no systematic change in variance is seen across the model realizations in either the 10-year IPO or 35-year AMV running trends (Figures S2a and S2b). This result conflicts with Murphy et al. (2017), who argue that historical forcings have enhanced AMV. However, their method of linearly detrending the historical simulations is known to create spurious variability (Frankcombe et al., 2015; Mann et al., 2014; Steinman et al., 2015).

### 4.2. Correlations Between GMST, IPO, and AMV Trends

To test the influence of large-scale patterns of variability on GMST, correlations were computed between the running trends of GMST and the IPO and AMV indices (Figures 1d and 1e). Almost all models simulate positive correlations between GMST and IPO trends, in agreement with observations, at shorter time scales (<25-year trends; Figure 1d), and between GMST and AMV trends at all time scales. Correlations of annual data in 31-year sliding windows also show that the relationship tends to be positive across models (Figures S2c and S2d). This finding appears to be inconsistent with Douville et al. (2015, their Figures 1c and 1d), who show a larger spread of positive and negative sliding correlations across models, for GMST with both Pacific Decadal Oscillation (PDO) and AMV. Douville et al. (2015) analyze PDO, but the difference between the PDO and IPO indices is small (Henley et al., 2015; Newman et al., 2016). The difference between our

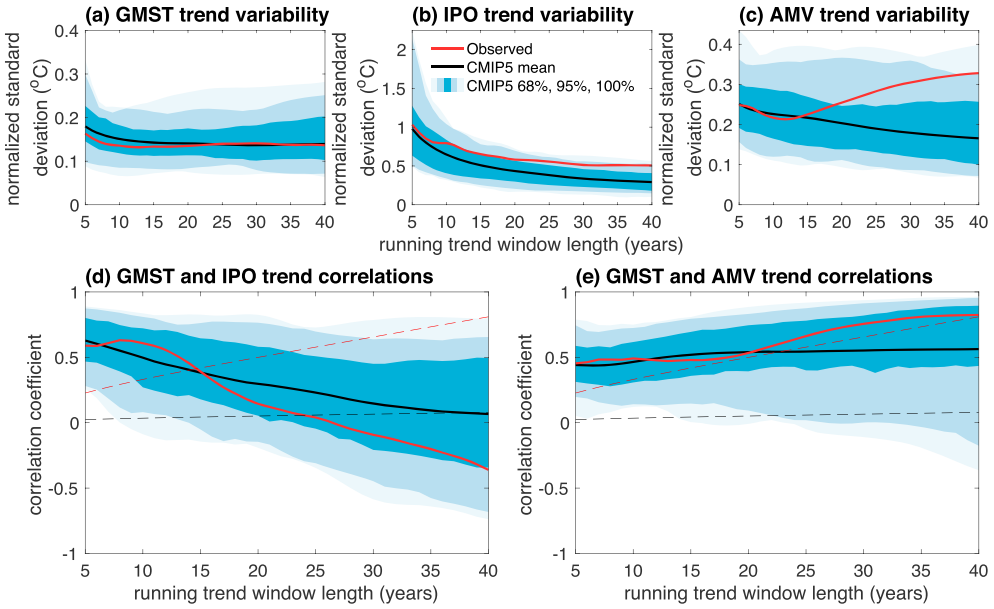


**Figure 1.** Standard deviation and correlations in the running trends of global mean surface temperature (GMST), the Interdecadal Pacific Oscillation (IPO), and the Atlantic Multidecadal Variability (AMV) indices. Standard deviation of running trend data, using a range of window lengths, for (a) GMST, (b) the IPO index, and (c) the AMV index, in observations and CMIP5 historical simulations. The shaded blue regions denote the central 68%, 95%, and 100% of the CMIP5 individual realization ensemble. For example, the darkest blue indicates the spread of the central 68% of realizations (more specifically, 59 out of 87 realizations). To better illustrate the variability on a linear *y* axis scale, the standard deviation was normalized by multiplying it with the running window length (in years), and hence, the units are °C. Correlations in running trends of GMST with (d) the IPO index and (e) the AMV index, using a range of window lengths. Dashed lines denote the 95% levels for statistically significant correlations (Text S3) for the observed data (red) and model data (black).

result and theirs highlights the need for more careful removal of the forced signal from observations and models. The biggest difference in procedures comes from their subtraction of each individual ensemble's global mean SST time series (rather than the multimodel mean). That step is avoided here because it is specifically those imprints of the large-scale patterns onto the global mean that are sought.

The observed relationship between GMST and IPO trends lies within the central 68% of the model spread, and the model-mean captures the diminishing correlation over longer time scales (Figure 1d). The GMST and IPO trend correlation peaks near the 10-year time scale in observations. Despite a statistically significant correlation for 10-year trends in more than 80% of model realizations, that same correlation maximum is not seen in most models. The strongest correlation occurs for five-year trends in 70% of realizations, and only two simulations exhibit a maximum correlation over 8-to-18-year time scales. A robust relationship between 10-year trends of GMST and IPO is also seen in the piControl CMIP5 simulations, where an IPO-like pattern emerges for the strongest cooling and warming decades (Middlemas & Clement, 2016).

Observed correlations in trends of GMST and AMV also lie within the central 68% model spread, but in this case the relationships do not diminish over longer time scales (Figure 1e). For observations, the strengthening of the GMST and AMV trend correlation may be a reflection of stronger AMV at longer time scales (Figure 1c). Although the multimodel mean correlation does not increase with time scale as strongly as it does in observations, the slight increase is nevertheless surprising, since the standard deviation of AMV tends to diminish with time scale in models (Figure 1c).

### 4.3. Intermodel Relationships Between GMST, IPO, and AMV

Here we explore whether there is any tendency for models simulating stronger IPO or AMV to also simulate stronger correlations with GMST. Analysis of 10-year trends for the IPO (Figure 2a), and 35-year trends for AMV (Figure 2b), suggests that indeed such relationships exists. The “intermodel correlation” is defined as the correlation across all of the available CMIP5 realizations between the index trend standard deviation (data shown in Figures 1b and 1c), and the correlation between trends in that index and GMST (data

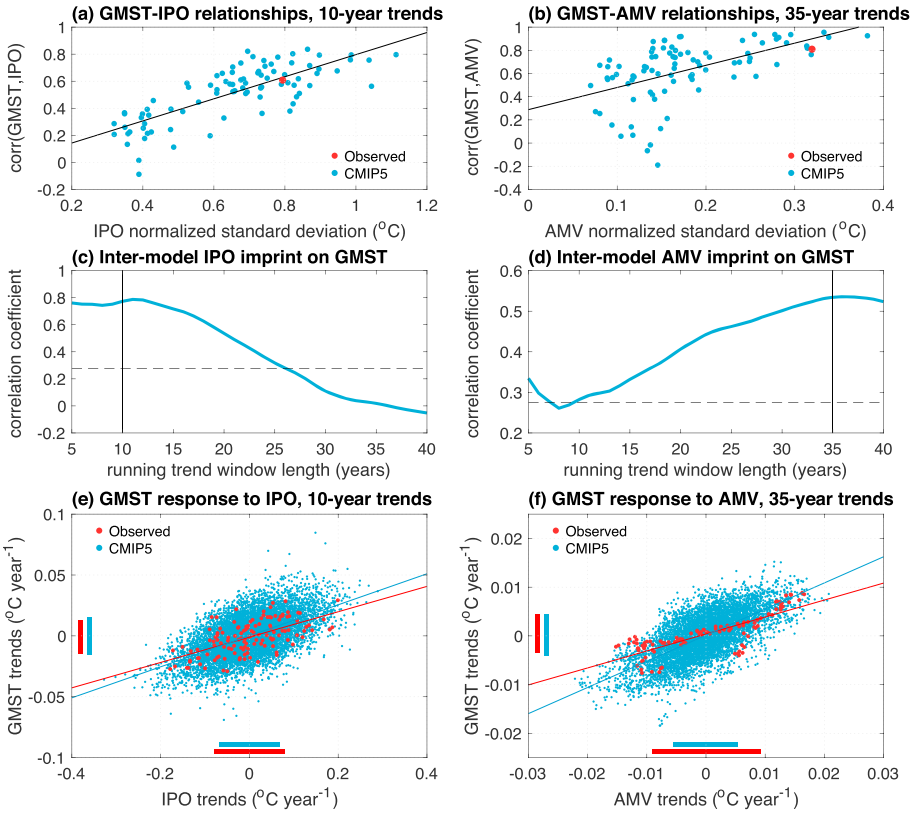


**Figure 2.** Relationships between running trends of global mean surface temperature (GMST), the Interdecadal Pacific Oscillation (IPO), and the Atlantic Multidecadal Variability (AMV) indices. (a) Relationship between the normalized standard deviation of the 10-year running trend in IPO index (Figure 1b), and the correlation between 10-year running trends of GMST and IPO index (Figure 1d). (b) Same as in (a), but for 35-year running trends of GMST and AMV index (Figures 1c and 1e). (c) The CMIP5 intermodel correlations of IPO standard deviation against GMST-IPO running trend correlations. For a given running trend window length, *N*, the *y* axis value denotes the correlation between two data sets: (i) the normalized standard deviation of the *N*-year running trend of IPO index in each CMIP5 realization and (ii) the correlation between *N*-year running trends of GMST and IPO index. For example, the vertical black line denotes the window length selected in (a), and thus, the value of 0.77 for 10-year trends denotes the correlation computed for the CMIP5 data in (a). The dashed line denotes the 99% levels for statistically significant intermodel correlations. (d) The CMIP5 intermodel correlations of AMV against GMST-AMV running trend correlations. The vertical black line denotes the window length selected in (b), and thus, the value of 0.53 for 35-year trends denotes the correlation computed for the CMIP5 data in (b). (e) Response of 10-year GMST trends to 10-year IPO index trends, in all CMIP5 historical realizations, and observations. The red (observed) and blue (CMIP5) lines denote the ordinary least squares fits to the data. The red (observed) and blue (CMIP5) horizontal and vertical bars denote the 1 standard deviation ranges in the data. (f) Same as in (e) but for 35-year trends in GMST and AMV index.

shown in Figures 1d and 1e). The intermodel correlation is 0.77 for the 10-year IPO trends (Figure 2a), and 0.53 for the 35-year AMV trends (Figure 2b). Both values are statistically significant above the 99% confidence level, implying that there is an overall tendency for models simulating stronger IPO at the 10-year time scale to also simulate a stronger relationship between IPO and GMST trends at that time scale, and likewise for AMV at the 35-year time scale.

The intermodel correlation may also be interpreted as a measure of the extent to which the patterns of variability "imprint" on GMST across the models. We next explored whether strong imprints of IPO and AMV onto GMST exist at all time scales (Figures 2c and 2d). The 10-year intermodel IPO imprint on GMST is indicated by a vertical line in Figure 2c (correlation of 0.77 in Figure 2a). Similarly, the 35-year intermodel AMV imprint on GMST is indicated by a vertical line in Figure 2d (correlation of 0.53 in Figure 2b). The strongest intermodel correlations emerge at those particular time scales, that is, decadal for the IPO, and multidecadal for AMV. Surprisingly, these tend to be the same time scales at which the IPO and AMV are strongest in observations, but not necessarily within all nor most models.

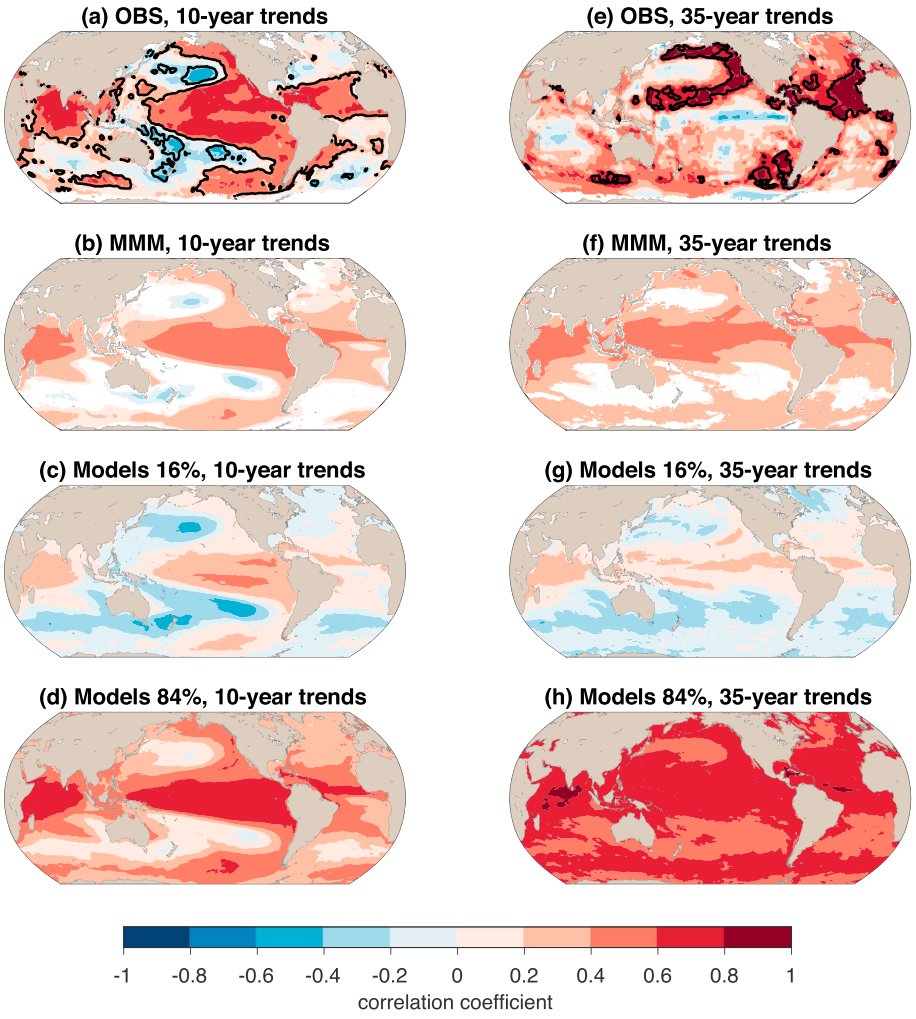


**Figure 3.** Correlations between running trends of global mean surface temperature (GMST) and grid-point sea surface temperature (SST). (a–d) 10-year running trends and (e–h) 35-year running trends, for (a and e) observations; (b and f) the multimodel mean (MMM) of the CMIP5 historical correlations; (c and g) the 16th percentile, at each grid point, of the correlations from the CMIP5 historical realization set; and (d and h) the 84th percentile. The forced response was first removed from GMST and from each SST grid point. For the observed data (a and e), the 95% statistical significance levels for correlations are indicated by black contours (Text S3). For the multimodel mean data (b and f), correlations are plotted only where at least 75% of the models agree on the sign.

Despite the model underrepresentation of decadal IPO and multidecadal AMV, there is good agreement between observed and modeled standard deviation of GMST trends (Figure 1a). The intermodel correlations would then appear to imply that if the models simulated more realistic IPO and AMV, they might then overrepresent GMST variability. To explore this discrepancy further, the sensitivity of GMST trends to IPO and AMV trends was tested (Figures 2e and 2f). Although the IPO standard deviation and GMST-IPO correlation are both stronger for 10-year trend data in observations, the sensitivity of GMST to IPO trends is weaker (exhibited by the slopes of ordinary least squares fits; Figure 2e). The result is similar, but clearer, for AMV (Figure 2f). In observed 35-year trends, a 1 °C/year trend in AMV corresponds with a 0.35 °C/year trend in GMST (i.e., $B = 0.35$ °C per °C). Across all of the model data, $B = 0.54$. Therefore, the overly strong sensitivity of 35-year GMST trends to AMV trends in models appears to play some role in offsetting their weaker standard deviation in AMV trends, thus resulting in GMST variability in the model mean that is close to the observed. It is unlikely that AMV sensitivity across models is solely responsible for the simulation of GMST trend variability similar to the observations, as the spatial patterns of correlations in the following section will show.

### 4.4. Spatial Maps of GMST and SST Correlations

Spatial correlations patterns between GMST trends and grid-point SST trends can help to identify the regions of strongest bias (Figure 3). Again, it is emphasized that this analysis is conducted with the forced signal removed from GMST and from each SST grid point. The familiar IPO-like patterns emerge at the 10-year trend time scale for both observations (Figure 3a) and in the multimodel mean of the correlations (Figure 3b). The weaker negative signatures in the North and South Pacific of the model pattern may explain the weaker-than-observed correlation between 10-year GMST and IPO index trends in the multimodel mean (Figure 1d). For 35-year trends, there are more striking differences between the observations (Figure 3e) and the model mean (Figure 3f). The strong positive correlation signal in the North Atlantic in observations (Figure 3e) is indicative of the relationship revealed in the AMV index analysis (Figure 1e). Although the model mean also exhibits positive correlations in the North Atlantic (Figure 3f), the global spatial pattern is more notably characterized by a strong positive signature across the tropics. To indicate the model spread in the correlations, the 16th and 84th percentiles (corresponding to the bounds of 1 standard deviation of a normal distribution), computed at each grid point from the CMIP5 ensemble set, are also shown (Figures 3c, 3d, 3g, and 3h). The positive correlations across the tropics for 35-year trends are exhibited by at least the central 68% of simulations (Figures 3g and 3h).

The multimodel mean correlation patterns of the CMIP5 piControl experiments are very similar to those in historical (Figure S3), which also provides some evidence that the forced response has been removed appropriately from the historical data. The spatial correlation patterns suggest that different processes are responsible for driving GMST trend changes at the multidecadal time scale across models and observations (Palmer & McNeall, 2014). The multidecadal North Atlantic influence on global climate is robust in observations (Chylek et al., 2016; Mann et al., 2014; O'Reilly et al., 2016; Wang et al., 2017), but GMST may respond more strongly to multidecadal tropical variability in models (Figure 3f).

## 5. Conclusions

After the removal of a reasonable estimate of the forced response, robust relationships between global mean surface temperature (GMST) changes and large-scale patterns of internal variability were found in observed data. GMST trends are most strongly correlated with trends in the Interdecadal Pacific Oscillation (IPO) on decadal time scales, and with Atlantic Multidecadal Variability (AMV) trends on multidecadal time scales. The range of standard deviations of GMST trends in CMIP5 historical simulations, also after forced response removal, are close to centered on the observations. However, models tend to exhibit weaker-than-observed standard deviation in IPO index trends at time scales of >10 years, and in AMV index trends at time scales of >20 years.

Observed correlations of GMST with IPO and AMV lie within the central 68% model spread, but the multimodel mean is weaker than observed at some time scales. The largest difference occurs at the ~10-year time scale for the IPO-GMST relationship, and at the ~35-year time scale for the AMV-GMST relationship. However, it was found that models simulating stronger IPO or AMV tend to also exhibit stronger correlations between GMST and IPO or AMV. Strikingly, the intermodel correlations are the strongest at the 10- and 35-year time scales. For example, models that show stronger standard deviation in 10-year trends of the IPO index tend to also show stronger correlations with GMST trends at that time scale. Likewise, models with greater standard deviation in 35-year trends of the AMV index tend to have stronger correlations between GMST and AMV trends.

An apparent paradox arises in this study: models underrepresent IPO and AMV, but multimodel mean internal GMST variability is close to observations across all time scales. At longer time scales, it was found that the underrepresentation of AMV in models is offset by stronger sensitivity of GMST to AMV, as compared to observations, thus providing a possible explanation for the discrepancy.

Apart from uncertainties related to the forced response removal, there are additional uncertainties related to this analysis. First, uncertainties in observed SSTs are larger prior to the satellite era, and increasingly so deeper in time (Huang et al., 2018). The conclusions drawn herein are consistent with other observational data sets, namely, GISTEMP (GISTEMP Team, 2018; Hansen et al., 2010) and ERSSTv5 (Huang et al., 2017), and also when the analysis is restricted to 1950–2017, a period for which the observational data is more robust

(Figure S4). Another potential uncertainty arises in the use of an area-averaged SST index to characterize the IPO, rather than, say, Empirical Orthogonal Functions. The fixed location SST index may not accurately capture the IPO in models if their centers of action are slightly displaced spatially, relative to the observations. While the multimodel mean of the GMST correlations with grid-point SST suggest that the IPO pattern overall agrees well with the observed (Figures 3a and 3b), this could be due to aliased variability in the pattern across the models (Henley et al., 2017).

Despite the robust relationships that have been revealed, it is not possible to infer from correlations alone whether the IPO and AMV are independent drivers of changes in GMST trends, or a response to, for example, top-of-atmosphere flux variations, or deep ocean changes (Hedemann et al., 2017). Further analysis is also required to identify the model biases that lead to weaker-than-observed IPO and AMV. However, spatial patterns of correlations suggest that different processes are responsible for driving GMST changes at multidecadal time scales across models and observations. In the model-mean, multidecadal GMST trends are more strongly correlated with SST trends in the tropics. Newman et al. (2016) find that linkages between the tropics and the PDO are different in observations and models, perhaps due to El Niño–Southern Oscillation model biases. Biases in simulations of AMV might be linked with underestimated variability in modeled Atlantic Meridional Overturning Circulation (Yan et al., 2018). Additionally, biases in cross-basin interactions may also contribute to diminished variability (Kajtar et al., 2018; McGregor et al., 2018). Nevertheless, this study provides a reasonable starting point for further efforts to identify biases that hamper simulations of large-scale variability.

**Acknowledgments**

This work was supported by the Natural Environment Research Council (SMURPHS project NE/N005783/1 and NE/N006348/1). L.M.F. was supported by the Australian Research Council (DE170100367). L.M.F. and M.H.E. were supported by the Australian Research Council's Centre of Excellence for Climate Extremes (CE17010023). We acknowledge the World Climate Research Programme's Working Group on Coupled Modeling, which is responsible for the Coupled Model Intercomparison Project (CMIP), and we thank the climate modeling groups for producing and making their model output available (http://pcmdi9.llnl.gov). We also thank the providers of the following observational data sets: HadISST v1.1 (https://www.metoffice.gov.uk/hadobs/hadisst), HadCRUT v4.5.0.0 (https://crudata.uea.ac.uk/cru/data/temperature), ERSST v5 (https://www.esrl.noaa.gov/psd/data/gridded/data.noaa.ersst.v5.html), and GISTEMP (https://data.giss.nasa.gov/gistemp/).

## References

Allen, M. R., & Stott, P. A. (2003). Estimating signal amplitudes in optimal fingerprinting, part I: Theory. *Climate Dynamics*, *21*(5-6), 477–491. https://doi.org/10.1007/s00382-003-0313-9

Cheung, A. H., Mann, M. E., Steinman, B. A., Frankcombe, L. M., England, M. H., & Miller, S. K. (2017). Comparison of low frequency internal climate variability in CMIP5 models and observations. *Journal of Climate*, *30*, 4763–4776. https://doi.org/10.1175/JCLI-D-16-0712.1

Chikamoto, Y., Mochizuki, T., Timmermann, A., Kimoto, M., & Watanabe, M. (2016). Potential tropical Atlantic impacts on Pacific decadal climate trends. *Geophysical Research Letters*, *43*, 7143–7151. https://doi.org/10.1002/2016GL069544

Chylek, P., Klett, J. D., Dubey, M. K., & Hengartner, N. (2016). The role of Atlantic multi-decadal oscillation in the global mean temperature variability. *Climate Dynamics*, *47*, 3271–3279. https://doi.org/10.1007/s00382-016-3025-7

Collins, M., Knutti, R., Arblaster, J. M., Dufresne, J.-L., Fichefet, T., Friedlingstein, P., et al. (2013). Long-term climate change: Projections, commitments and irreversibility. In *Climate Change 2013: The Physical Science Basis. Contribution of Working Group I to the Fifth Assessment Report of the Intergovernmental Panel on Climate Change* (pp. 1029–1136). Cambridge, United Kingdom and New York: Cambridge University Press.

Cowtan, K., Hausfather, Z., Hawkins, E., Jacobs, P., Mann, M. E., Miller, S. K., et al. (2015). Robust comparison of climate models with observations using blended land air and ocean sea surface temperatures. *Geophysical Research Letters*, *42*, 6526–6534. https://doi.org/10.1002/2015GL064888

Dai, A., Fyfe, J. C., Xie, S.-P., & Dai, X. (2015). Decadal modulation of global surface temperature by internal climate variability. *Nature Climate Change*, *5*, 555–559. https://doi.org/10.1038/nclimate2605

Dong, L., & Zhou, T. (2014). The formation of the recent cooling in the eastern tropical Pacific Ocean and the associated climate impacts: A competition of global warming, IPO, and AMO. *Journal of Geophysical Research: Atmosphere*, *119*, 11,272–11,287. https://doi.org/10.1002/2013JD021395

Douville, H., Voldoire, A., & Geoffroy, O. (2015). The recent global warming hiatus: What is the role of Pacific variability? *Geophysical Research Letters*, *42*, 880–888. https://doi.org/10.1002/2014GL062775

England, M. H., Kajtar, J. B., & Maher, N. (2015). Robust warming projections despite the recent hiatus. *Nature Climate Change*, *5*, 394–396. https://doi.org/10.1038/nclimate2575

England, M. H., McGregor, S., Spence, P., Meehl, G. A., Timmermann, A., Cai, W., et al. (2014). Recent intensification of wind-driven circulation in the Pacific and the ongoing warming hiatus. *Nature Climate Change*, *4*, 222–227. https://doi.org/10.1038/nclimate2106

Farneti, R. (2017). Modelling interdecadal climate variability and the role of the ocean. *Wiley Interdisciplinary Reviews: Climate Change*, *8*, e441. https://doi.org/10.1002/wcc.441

Flato, G., Marotzke, J., Abiodun, B., Braconnot, P., Chou, S. C., Cox, W. C. P., et al. (2013). Evaluation of climate models. In *Climate Change 2013: The Physical Science Basis. Contribution of Working Group I to the Fifth Assessment Report of the Intergovernmental Panel on Climate Change* (pp. 741–866). Cambridge: Cambridge University Press.

Frankcombe, L. M., England, M. H., Kajtar, J. B., Mann, M. E., & Steinman, B. A. (2018). On the choice of ensemble mean for estimating the forced signal in the presence of internal variability. *Journal of Climate*, *31*, 5681–5693. https://doi.org/10.1175/JCLI-D-17-0662.1

Frankcombe, L. M., England, M. H., Mann, M. E., & Steinman, B. A. (2015). Separating internal variability from the externally forced climate response. *Journal of Climate*, *28*, 8184–8202. https://doi.org/10.1175/JCLI-D-15-0069.1

GISTEMP Team (2018). GISS Surface Temperature Analysis (GISTEMP). Retrieved from http://www.data.giss.nasa.gov/gistemp/. Dataset accessed 2019-01-15.

Hansen, J. E., Ruedy, R., Sato, M., & Lo, K. (2010). Global surface temperature change. *Reviews of Geophysics*, *48*, RG4004. https://doi.org/10.1029/2010RG000345

Hedemann, C., Mauritsen, T., Jungclaus, J. H., & Marotzke, J. (2017). The subtle origins of surface-warming hiatuses. *Nature Climate Change*, *7*, 336–339. https://doi.org/10.1038/nclimate3274

Henley, B. J., Gergis, J., Karoly, D. J., Power, S., Kennedy, J., & Folland, C. K. (2015). A tripole index for the Interdecadal Pacific Oscillation. *Climate Dynamics*, *45*, 3077–3090. https://doi.org/10.1007/s00382-015-2525-1

Henley, B. J., & King, A. D. (2017). Trajectories towards the 1.5 °C Paris target: Modulation by the Interdecadal Pacific Oscillation. *Geophysical Research Letters*, *44*, 4256–4262. https://doi.org/10.1002/2017GL073480

Henley, B. J., Meehl, G. A., Power, S. B., Folland, C. K., King, A. D., Brown, J. N., et al. (2017). Spatial and temporal agreement in climate model simulations of the Interdecadal Pacific Oscillation. *Environmental Research Letters*, *12*, 044011. https://doi.org/10.1088/1748-9326/aa5cc8

Huang, B., Angel, W., Boyer, T., Cheng, L., Chepurin, G., Freeman, E., et al. (2018). Evaluating SST analyses with independent ocean profile observations. *Journal of Climate*, *31*, 5015–5030. https://doi.org/10.1175/JCLI-D-17-0824.1

Huang, B., Thorne, P. W., Banzon, V. F., Boyer, T., Chepurin, G., Lawrimore, J. H., et al. (2017). Extended Reconstructed Sea surface temperature version 5 (ERSSTv5): Upgrades, validations, and intercomparisons. *Journal of Climate*, *30*, 8179–8205. https://doi.org/10.1175/JCLI-D-16-0836.1

Huber, M., & Knutti, R. (2014). Natural variability, radiative forcing and climate response in the recent hiatus reconciled. *Nature Geoscience*, *7*, 651–656. https://doi.org/10.1038/ngeo2228

Kajtar, J. B., Santoso, A., McGregor, S., England, M. H., & Baillie, Z. (2018). Model under-representation of decadal Pacific trade wind trends and its link to tropical Atlantic bias. *Climate Dynamics*, *50*, 1471–1484. https://doi.org/10.1007/s00382-017-3699-5

Knight, J. R. (2009). The Atlantic multidecadal oscillation inferred from the forced climate response in coupled general circulation models. *Journal of Climate*, *22*(7), 1610–1625. https://doi.org/10.1175/2008JCLI2628.1

Kosaka, Y., & Xie, S.-P. (2013). Recent global-warming hiatus tied to equatorial Pacific surface cooling. *Nature*, *501*, 403–407. https://doi.org/10.1038/nature12534

Kosaka, Y., & Xie, S.-P. (2016). The tropical Pacific as a key pacemaker of the variable rates of global warming. *Nature Geoscience*, *9*, 669–673. https://doi.org/10.1038/ngeo2770

Li, X.-C., Xie, S.-P., Gille, S. T., & Yoo, C. (2016). Atlantic-induced pan-tropical climate change over the past three decades. *Nature Climate Change*, *6*, 275–279. https://doi.org/10.1038/nclimate2840

Luo, J.-J., Sasaki, W., & Masumoto, Y. (2012). Indian Ocean warming modulates Pacific climate change. *Proceedings of the National Academy of Sciences*, *109*, 18,701–18,706. https://doi.org/10.1073/pnas.1210239109

Lyu, K., & Yu, J.-Y. (2017). Climate impacts of the Atlantic multidecadal oscillation simulated in the CMIP5 models: A re-evaluation based on a revised index. *Geophysical Research Letters*, *44*, 3867–3876. https://doi.org/10.1002/2017GL072681

Maher, N., Sen Gupta, A., & England, M. H. (2014). Drivers of decadal hiatus periods in the 20th and 21st centuries. *Geophysical Research Letters*, *41*, 5978–5986. https://doi.org/10.1002/2014GL060527

Mann, M. E., Steinman, B. A., & Miller, S. K. (2014). On forced temperature changes, internal variability, and the AMO. *Geophysical Research Letters*, *41*, 3211–3219. https://doi.org/10.1002/2014GL059233

Marotzke, J., & Forster, P. M. (2015). Forcing, feedback and internal variability in global temperature trends. *Nature*, *517*, 565–570. https://doi.org/10.1038/nature14117

McGregor, S., Stuecker, M. F., Kajtar, J. B., & England, M. H. (2018). Model tropical Atlantic biases underpin diminished Pacific decadal variability. *Nature Climate Change*, *8*, 493–498. https://doi.org/10.1038/s41558-018-0163-4

McGregor, S., Timmermann, A., Stuecker, M. F., England, M. H., Merrifield, M., Jin, F. F., & Chikamoto, Y. (2014). Recent Walker circulation strengthening and Pacific cooling amplified by Atlantic warming. *Nature Climate Change*, *4*, 888–892. https://doi.org/10.1038/nclimate2330

Medhaug, I., Stolpe, M. B., Fischer, E. M., & Knutti, R. (2017). Reconciling controversies about the "global warming hiatus". *Nature*, *545*, 41–47. https://doi.org/10.1038/nature22315

Meehl, G. A., Hu, A., Santer, B. D., & Xie, S.-P. (2016). Contribution of the Interdecadal Pacific Oscillation to twentieth-century global surface temperature trends. *Nature Climate Change*, *6*, 1005–1008. https://doi.org/10.1038/nclimate3107

Middlemas, E. A., & Clement, A. C. (2016). Spatial patterns and frequency of unforced decadal-scale changes in global mean surface temperature in climate models. *Journal of Climate*, *29*, 6245–6257. https://doi.org/10.1175/JCLI-D-15-0609.1

Morice, C. P., Kennedy, J. J., Rayner, N. A., & Jones, P. D. (2012). Quantifying uncertainties in global and regional temperature change using an ensemble of observational estimates: The HadCRUT4 data set. *Journal of Geophysical Research*, *117*, D08101. https://doi.org/10.1029/2011JD017187

Murphy, L. N., Bellomo, K., Cane, M. A., & Clement, A. C. (2017). The role of historical Forcings in simulating the observed Atlantic multidecadal oscillation. *Geophysical Research Letters*, *44*, 2472–2480. https://doi.org/10.1002/2016GL071337

Nagy, M., Petrovay, K., & Erdélyi, R. (2017). The Atlanto-Pacific multidecade oscillation and its imprint on the global temperature record. *Climate Dynamics*, *48*, 1883–1891. https://doi.org/10.1007/s00382-016-3179-3

Newman, M., Alexander, M. A., Ault, T. R., Cobb, K. M., Deser, C., di Lorenzo, E., et al. (2016). The Pacific decadal oscillation, revisited. *Journal of Climate*, *29*, 4399–4427. https://doi.org/10.1175/JCLI-D-15-0508.1

Oka, A., & Watanabe, M. (2017). The post-2002 global surface warming slowdown caused by the subtropical Southern Ocean heating acceleration. *Geophysical Research Letters*, *44*, 3319–3327. https://doi.org/10.1002/2016GL072184

O'Reilly, C. H., Huber, M., Woollings, T., & Zanna, L. (2016). The signature of low-frequency oceanic forcing in the Atlantic multidecadal oscillation. *Geophysical Research Letters*, *43*, 2810–2818. https://doi.org/10.1002/2016GL067925

Palmer, M. D., & McNeall, D. J. (2014). Internal variability of Earth's energy budget simulated by CMIP5 climate models. *Environmental Research Letters*, *9*, 034016. https://doi.org/10.1088/1748-9326/9/3/034016

Pasini, A., Triacca, U., & Attanasio, A. (2017). Evidence for the role of the Atlantic multidecadal oscillation and the ocean heat uptake in hiatus prediction. *Theoretical and Applied Climatology*, *129*, 873–880. https://doi.org/10.1007/s00704-016-1818-6

Rayner NA, Parker DE, Horton EB, Folland Chris K., Alexander Lisa V., Rowell David, et al. (2003). Global analyses of sea surface temperature, sea ice, and night marine air temperature since the late nineteenth century. *Journal of Geophysical Research 108*, 3824. https://doi.org/10.1029/2002JD002670

Riahi, K., Rao, S., Krey, V., Cho, C., Chirkov, V., Fischer, G., et al. (2011). RCP 8.5—A scenario of comparatively high greenhouse gas emissions. *Climatic Change*, *109*, 33–57. https://doi.org/10.1007/s10584-011-0149-y

Santer, B. D., Bonfils, C., Painter, J. F., Zelinka, M. D., Mears, C., Solomon, S., et al. (2014). Volcanic contribution to decadal changes in tropospheric temperature. *Nature Geoscience*, *7*, 185–189. https://doi.org/10.1038/ngeo2098

Schmidt, G. A., Shindell, D. T., & Tsigaridis, K. (2014). Reconciling warming trends. *Nature Geoscience*, *7*, 158–160. https://doi.org/10.1038/ngeo2105

Schurer, A. P., Hegerl, G. C., Mann, M. E., Tett, S. F. B., & Phipps, S. J. (2013). Separating forced from chaotic climate variability over the past millennium. *Journal of Climate*, *26*, 6954–6973. https://doi.org/10.1175/JCLI-D-12-00826.1

Sen Gupta, A., Jourdain, N. C., Brown, J. N., & Monselesan, D. P. (2013). Climate drift in the CMIP5 models. *Journal of Climate*, *26*, 8597–8615. https://doi.org/10.1175/JCLI-D-12-00521.1

Smith, D. M., Booth, B. B. B., Dunstone, N. J., Eade, R., Hermanson, L., Jones, G. S., et al. (2016). Role of volcanic and anthropogenic aerosols in the recent global surface warming slowdown. *Nature Climate Change*, *6*, 936–940. https://doi.org/10.1038/nclimate3058

Steinman, B. A., Mann, M. E., & M. S. K. (2015). Atlantic and Pacific multidecadal oscillations and northern hemisphere temperatures. *Science*, *347*, 2269–2272.

Stolpe, M. B., Medhaug, I., & Knutti, R. (2017). Contribution of Atlantic and Pacific multidecadal variability to twentieth century temperature changes. *Journal of Climate*, *30*, 6279–6295. https://doi.org/10.1175/JCLI-D-16-0803.1

Trenberth, K. E., & Shea, D. J. (2006). Atlantic hurricanes and natural variability in 2005. *Geophysical Research Letters*, *33*, L12704. https://doi.org/10.1029/2006GL026894

Vecchi, G. A., Delworth, T. L., & Booth, B. B. B. (2017). Climate science: Origins of Atlantic decadal swings. *Nature*, *548*(7667), 284–285. https://doi.org/10.1038/nature23538

Vernier, J. P., Thomason, L. W., Pommereau, J. P., Bourassa, A., Pelon, J., Garnier, A., et al. (2011). Major influence of tropical volcanic eruptions on the stratospheric aerosol layer during the last decade. *Geophysical Research Letters*, *38*, L12807. https://doi.org/10.1029/2011GL047563

Wang, J., Yang, B., Ljungqvist, F. C., Luterbacher, J., Osborn, T. J., Briffa, K. R., & Zorita, E. (2017). Internal and external forcing of multidecadal Atlantic climate variability over the past 1,200 years. *Nature Geoscience*, *10*, 512–517. https://doi.org/10.1038/ngeo2962

Watanabe, M., Shiogama, H., Tatebe, H., Hayashi, M., Ishii, M., & Kimoto, M. (2014). Contribution of natural decadal variability to global warming acceleration and hiatus. *Nature Climate Change*, *4*, 893–897. https://doi.org/10.1038/nclimate2355

Yan, X., Zhang, R., & Knutson, T. R. (2018). Underestimated AMOC variability and implications for AMV and predictability in CMIP models. *Geophysical Research Letters*, *45*, 4319–4328. https://doi.org/10.1029/2018GL077378

Yao, S.-L., Huang, G., Wu, R., & Qu, X. (2016). The global warming hiatus—A natural product of interactions of a secular warming trend and a multi-decadal oscillation. *Theoretical and Applied Climatology*, *123*, 349–360. https://doi.org/10.1007/s00704-014-1358-x